ELSEVIER

PII: S0032-3861(97)00479-5

Polymer Vol. 39 No. 17, pp. 4089–4094, 1998

0032-3861/98/$19.00+0.00

Block copolymers based on nylon 6 and poly(propylene glycol). I. Structure and thermal properties

K. Sakurai*, G. Amador and T. Takahashi
Fukui University, Department of Materials Science and Engineering, Faculty of Engineering, Fukui 910, Japan
(Received 9 January 1997; revised 20 May 1997; accepted 30 May 1997)

The structure and the thermal properties of nylon 6-poly(propylene glycol) block copolymers have been studied using DSC, WAXD, SAXS, POM and DMA measurements and compared with those of nylon 6 homopolymer. The soft segment was found to be compatible with the hard segment in the armorphous region of block copolymers. The hard segment can partially crystallize and forms the same crystal structure as nylon 6. The melting point depression might be predicted by using Flory's model for random copolymers but the heat of fusion for crystals of the block copolymer with a large amount of soft segment (PAE-48) was much reduced than the value expected from the hard segment content. On annealing, the second lower melting temperature which increased linearly with the annealing temperature appeared in addition to the constant high melting temperature. The d_{200} spacing of the intermolecular hydrogen-bonded plane approached that of the ideal crystal at relatively low annealing temperatures in the block copolymers. The soft segment of block copolymer was suggested to exist in the amorphous layers between the stacked lamellar crystals.

(Keywords: block copolymers; compatibility; melting points)

INTRODUCTION

Thermoplastic elastomers (TPE) have special characteristics such as suitable solvent resistance, good mechanical properties and processibility[1,2]. Nylon 6-poly(propyleneglycol)-based block copolymers consist of hard and soft segments whose interactions in the phase structure and boundaries give the properties of TPE[1,3]. The general chemical structure of these polyamide elastomers is shown in *Figure 1*. The hard segment of polyamide crystallizes from the melt under suitable conditions[2], leading to a thermally reversible network structure which contributes to a dimensional stability of TPE. On the contrary, the polyether or soft segment (PPG) has a low glass transition temperature and forms a liquid-like phase, which gives the elastomeric character of these block copolymers at room temperature[2–4].

The composition ratio of polyether and polyamide is one of the main factors that control the properties of the block copolymer. For example, Goldback *et al.*[3] found that the content of the soft segment strongly affected the volume–strain and stress–strain behaviors in the alloy system of polylaurolactam (polyamide 12) and segmented polylaurolactam.

In the present research, the structures and thermal properties have been studied using the wide-angle and small-angle X-ray techniques, polarized optical microscopy, differential scanning calorimetry and dynamic mechanical analysis.

EXPERIMENTAL

Materials

The polymers used throughout this study were nylon 6 (Ny 6) and multi-block copolymers with 67% (PAE-67) and 48% (PAE-48) of polyamide content. The block copolymers were made by condensation polymerization of HOOC–R′–COOH (R′: nylon 6 oligomer with the average molecular weight of $M_w \cong 400$ for PAE-67 and $M_w \cong 1800$ for PAE-48, which could be calculated by assuming them to be alternative multi block copolymers) and H_2N–$(RO)_n$–NH_2 [$(RO)_n$: polypropyrene glycol oligomer with the average molecular weight of $M_w \cong 2000$].

Pellets of Ny 6 and block copolymers were dried in a vacuum oven at 120°C for 3 h. Films were made by molding the pellet samples at the temperature 30°C higher than the melting temperature, $(T_m + 30)$°C, under a pressure of about 50×10^5 Pa for 3 min and then quenched in water at room temperature. Annealed samples were also prepared in an oil bath at various temperatures.

Measurements

Differential Scanning Calorimeter (DSC). Measurements were performed with a Seiko DSC 200 differential

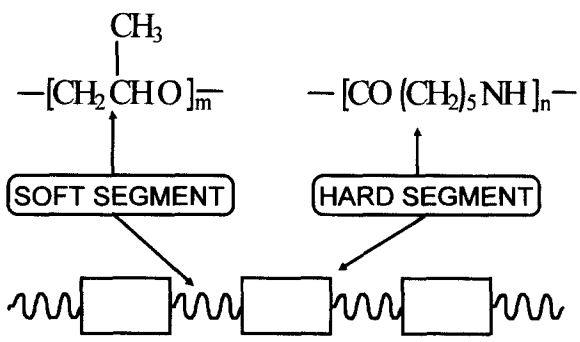

Figure 1 Chemical structure of nylon 6-poly(propylene glycol) block copolymers

* To whom correspondence should be addressed

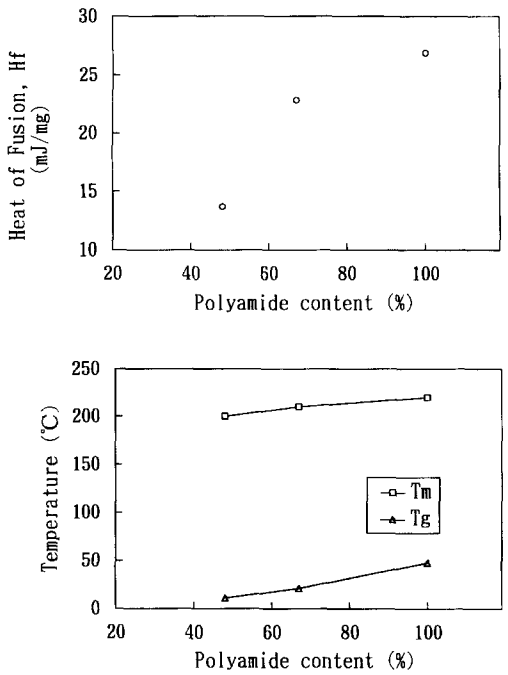

Figure 2 Heat of fusion, melting temperature, T_m, and glass transition temperature, T_g, of the quenched samples, estimated from DSC thermograms in the second heating run

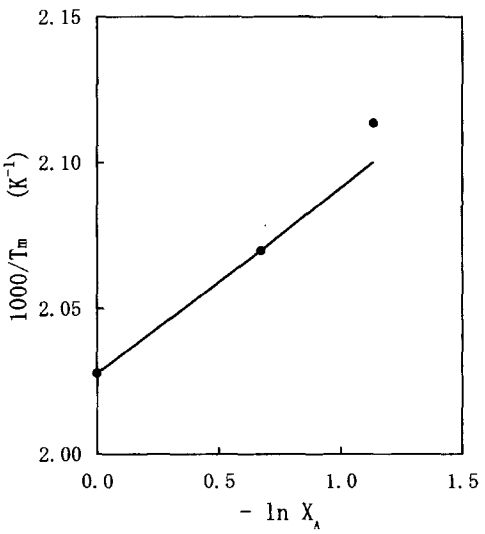

Figure 3 A plot of the reciprocal of the melting temperature against -lnX_A

scanning calorimeter, at a constant heating and cooling rate of 10 K/min in two cycles with a temperature range from −50°C to ca. 250°C.

The melting temperature, T_m, of each sample was determined from the maximum of the melting peak. The glass transition temperature, T_g, was taken as the onset of change of slope in the DSC thermogram.

Polarized optical microscope (POM). Observations were carried out with an Olympus BH2 polarized optical microscope. The sample films observed were prepared as follows: a few pellets of the sample were melted on a slide glass at (T_m + 30)°C, spread out on it with a cover glass to make a thin film, kept at the same temperature for 5 min and then isothermally crystallized at (T_m − 30)°C for 1 h.

Wide-angle X-ray diffraction (WAXD). Wide-angle X-ray diffractograms were obtained with a Rigaku Denki D-IA X-ray diffractometer equipped with a scintillation counter, utilizing nickel-filtered CuK_α radiation at 35 kV, 18 mA.

Small-angle X-ray scattering (SAXS). SAXS patterns were obtained using a JEOL JRX-12 VA generator with a photographic attachment, utilizing nickel filtered CuK_α radiation at 40 kV and 300 mA. The long period was evaluated from the position of SAXS intensity maximum on the photograph and the camera length by use of the Bragg's equation.

Dynamic–mechanical analysis (DMA). Measurements were carried out with Rheometric Scientific RSA II in a temperature range from −50°C to a temperature just below the melting point of each sample. They were made at a constant frequency of 1 Hz to obtain the mechanical loss tangent, tan δ, curves for the samples annealed at (T_m − 30)°C.

RESULTS AND DISCUSSION

DSC and DMA results

Figure 2 shows the thermal behavior of the quenched samples measured by DSC. From the heat of fusion, we can see that crystallinity diminishes as the amount of soft segment increases. Especially, PAE-48 has a large reduction in the heat of fusion, i.e. the crystallinity in PAE-48 is extremely lower than the value expected from the polyamide content. At the same time, the melting temperature (T_m) and the glass transition temperature (T_g) decrease monotonously. The depression of melting point is mainly due (a) to the 'diluent effect', which is dependent on the mole fraction of the crystallizable component in the copolymer, proposed by Flory[5], although Flory's theory was first developed for a random copolymer, and (b) to the crystal size limitations owing to the hindrance of the soft segment, in which the melting point is proportional to the reciprocal of the crystal thickness, provided by Hoffman and Weeks[6]. The depression of melting point has been discussed in some poly-ester-ethers block copolymers[7–10], in which the concept of 'diluent effect' gave a good interpretation.

Flory's equation is expressed as follows:

$$\frac{1}{T_m} - \frac{1}{T_m^\circ} = -\left(\frac{R}{\Delta H_f}\right) \ln X_A \qquad (1)$$

where T_m and T_m° are the melting temperatures of the copolymer and the homopolymer A of hard segments, respectively, X_A is the mole fraction of hard segments in the copolymer, ΔH_f is the heat of fusion of homopolymer A and R is the gas constant. If the melting temperature depression were determined by the 'diluent effect', the relation of $1/T_m \propto -\ln X_A$ would be expected. This analysis needs the mole fraction of hard segments, X_A, to be known but it can be calculated from the following equation under the assumption that the sample is an alternative multi block copolymer with the molecular weight distributed in a narrow range, as mentioned above.

$$X_A = \frac{w}{w + \frac{M_A}{M_B}(1-w)} \qquad (2)$$

where w is the weight fraction of hard segments, M_A and M_B

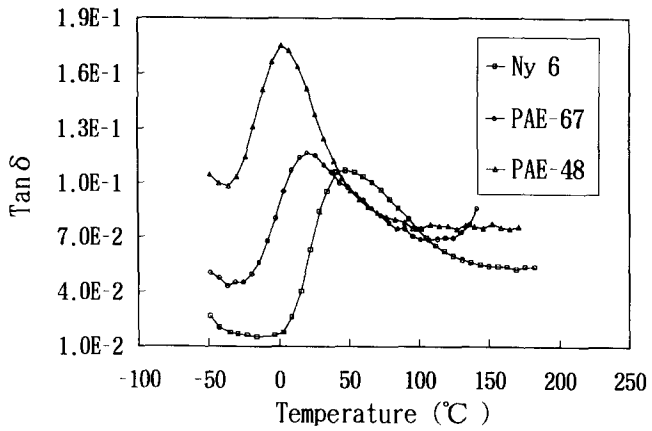

Figure 4 Loss tangent, tan δ, of samples annealed at $(T_m - 30)$°C as a function of temperature

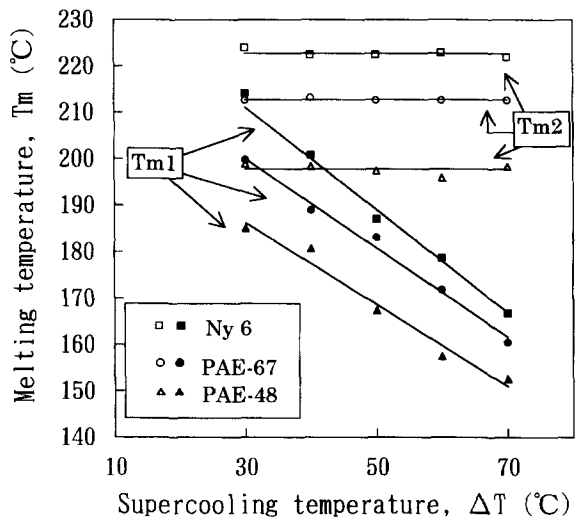

Figure 5 Two melting temperatures of annealed samples, estimated from DSC thermograms in the first heating run, as a function of supercooling temperature, $\Delta T = T_m - T_a$

are the molecular weight of the repeat unit of the hard and soft segments, respectively. The reciprocal of the melting temperature, $1/T_m$, was plotted against $-\ln X_A$ in *Figure 3*, in which the value of X_A was calculated by equation (2). The result shows almost linear relationship, indicating that the melting point depression almost obeys the diluent effect, although the melting temperature of PAE-48 is slightly deviated to the lower temperature than that expected from this effect. PAE-48 may also be subjected to small effects of the crystal size limitations and/or crystal defects. On the contrary, the result obtained in *Figure 3* can be considered to support the validity of the assumption mentioned above.

On the other hand, the glass transition temperature of nylon 6 is reported to be 48°C, estimated from DSC measurements and to be 65°C or 75°C, from the tan δ peaks of viscoelastic measurements[11]. The glass transition temperature of polypropyrene glycol is not known but that of polyethylene glycol is reported to be ~7°C[12], whose value may be assumed to be a little lower than that of the former. Taking these T_g values into account, the change of the glass transition temperatures with the content of soft segment demonstrates that the polyether and polyamide units are markedly compatible in the amorphous region, possibly due to the interactions between the NH groups of the hard segments and ether groups of soft segments[1,13].

The mechanical loss tangent, tan δ, of the annealed samples are shown in *Figure 4*. According to Prevoserk and co-workers[14], aliphatic polyamides have the three mechanical relaxations in the temperature range between 120 and −150°C, i.e. the α, β and γ relaxations observed at about 80, −40 and −120°C, respectively. The α relaxation temperature correspondings to T_g and its magnitude in the tan δ curve represents the relative amount of the amorphous phase undergoing the transition to the rubbery state[1]. PAE-48 shows the greatest magnitude of tan δ peak, which reflects the largest content of soft segment of the three samples. The most important fact obtained here is that the T_g value moves from approximately 50°C to approximately 0°C as the content of soft segment increases. This result coincides well with the T_g variation, estimated from DSC measurements, as shown in *Figure 2*, through the tan δ peak is somewhat broad and the T_g values are a little lower than the reference values.

The effect of annealing temperature on the melting points of the samples can be seen in *Figure 5*, where the two melting peaks appear; the lower melting temperature is designated as 'T_{m1}' and the higher one as 'T_{m2}' and besides the supercooling temperature, ΔT, is defined here as the difference between the melting temperature of the individual quenched sample and the annealing temperature $(= T_m - T_a)$. ΔT can be a more suitable parameter than the absolute value of T_a for discussing the annealing effect on each sample with the distinct T_m. In any samples T_{m1} increases linearly with decrease of ΔT while T_{m2} remains basically constant, though both melting temperatures depend on the content of hard segments in the same way as seen in the quenched samples. These results lead that T_{m1} corresponds to the melting of imperfect crystals with the smaller crystal thickness, which are formed by crystallization during cooling after the annealing process[1]. As is well known[15], an annealed polymer has a stabler crystal structure than a quenched one. The higher melting peak, T_{m2}, thus, corresponds to the melting point of the stable crystal. Similar melting behaviors have been found in other crystalline polymers such as PET, PEEK and PPS[16–18].

WAXD results

Figure 6 shows WAXD intensity curves of Ny 6 and both copolymers of PAE-67 and PAE-48. Quenched specimens of three samples show only one intensity peak at approximately $2\theta = 21.4°$, which could be a result of the superposition of the amorphous halo and the crystalline diffraction due to the γ-form crystal of nylon 6[19–21] in the polyamide domains of hard segments. When the annealing temperature is elevated, the crystal begins to transform to the α-form crystal at about $(T_m - 50)$°C and the transformation is completed at $(T_m - 10)$°C in every sample. Here, the α-form of nylon 6 is characterized by the two equatorial reflections, i.e. the (200) reflection at the scattering angle of about 20° and the (002) and (202) reflections at about 23.8°[1,19–24]. Thus it was found that the α-form crystal of nylon 6 was formed in the polyamide domains of these block copolymers like some other poly(either-block-amide) polymers, which gave rise to the same crystal structure as that of the corresponding polyamide homopolymer[1,24,25].

In order to estimate the degree of perfection of the crystal lattice by annealing, the d-spacing was calculated from the WAXD intensity curve using Bragg's equation for the scattering angle at the intensity maximum. The results appear in *Figure 7*. All samples showed a similar tendency:

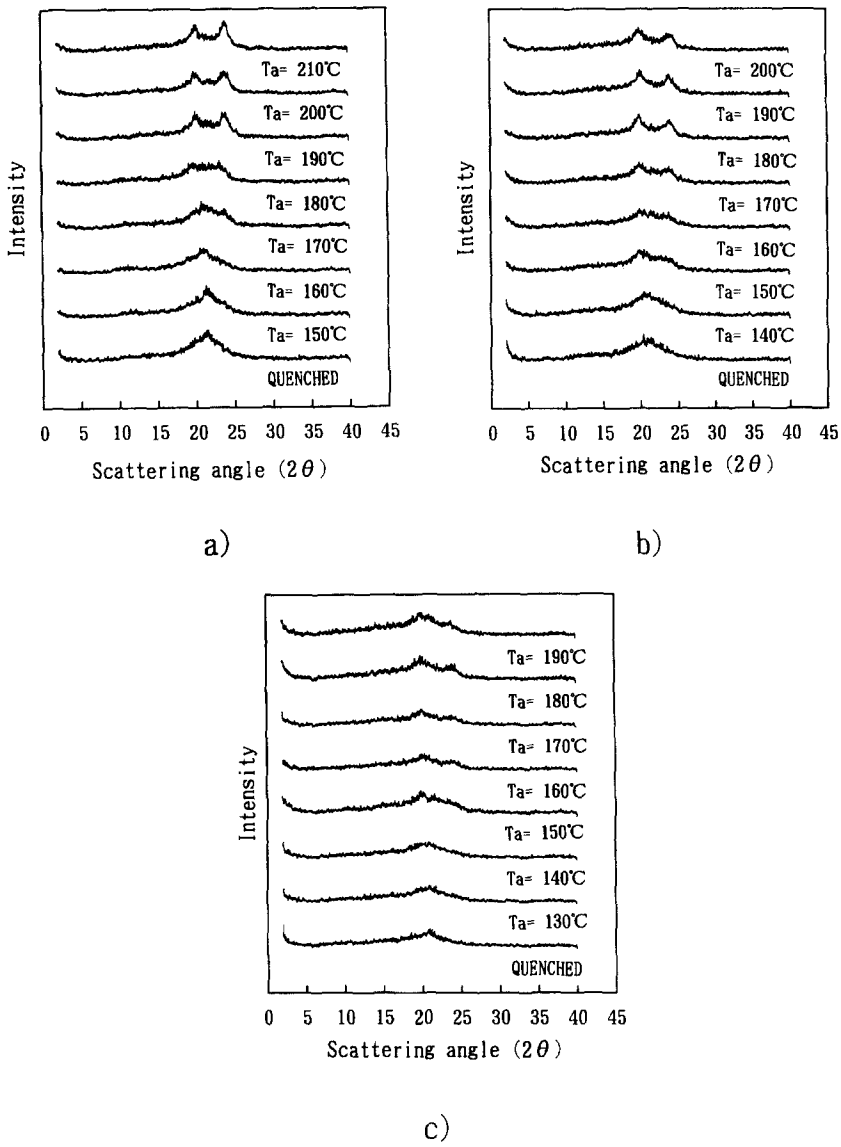

Figure 6 WAXD intensity curves of (a) Ny 6, (b) PAE-67 and (c) PAE-48 annealed at various temperatures

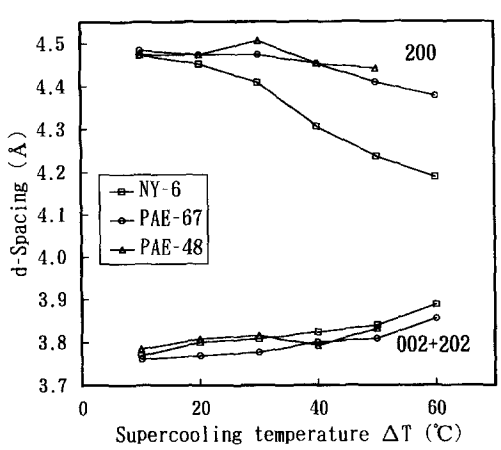

Figure 7 Spacings of d_{200} and $d_{002+202}$ of annealed samples as a function of supercooling temperature, $\Delta T = T_m - T_a$

the lower the supercooling temperature, $\Delta T = T_m - T_a$, the higher the d_{200} spacing and the lower the $d_{002+202}$ spacing. In other words, as T_a increases the molecular chains of nylon 6 domains are packed in a more stable conformation so that the crystal structure approaches to the ideal α-form. When the annealing effect on the change of d-spacing is carefully inspected, ΔT has almost the same effect for the $d_{002+202}$ spacings in three samples but has a different effect for the d_{200} spacings; it should be noted that the d_{200} spacings of PAE-67 and PAE-48 are higher than those of Ny 6 at high ΔT values. This may be a result of a 'plasticizing effect' of the soft segments that enhances the mobility of molecular chains in the block copolymer. It allows that the molecular chains take a more stable arrangement in nylon 6 crystal lattice at high ΔT, since the (200) planes are connected to each other by the intermolecular hydrogen bonds.

Attention is now paid to the widths of the (200) and (002) + (202) reflections shown in *Figure 6*, which are related to the size of crystallites[26] in the direction of a- and c-axes of the crystallites. Comparing the three samples annealed at the highest temperatures of (T_m-10)°C, PAE-48 has the broadest peak widths and PAE-67 has a little broader one than Ny 6. This means that PAE-67 has larger crystallites, similar to those of Ny 6, than PAE-48, which possesses the smallest crystallites in the direction along the ac plane of the crystallites. The similar results were obtained by the POM observations, shown in *Figure 8*, where all samples

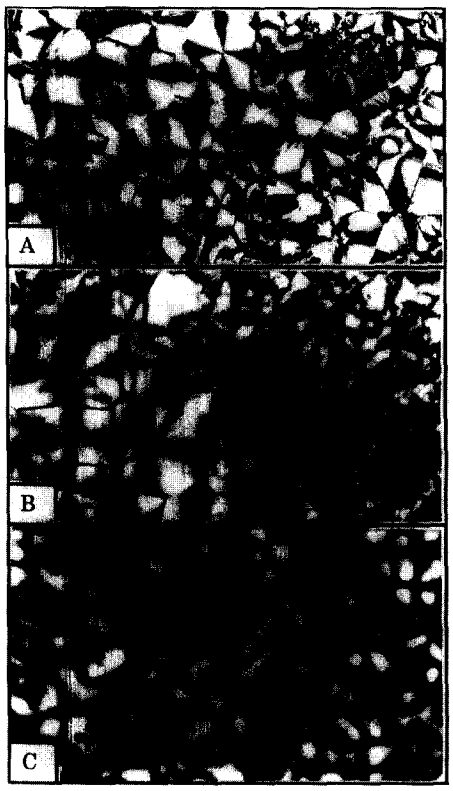

Figure 8 Cross-polarized optical microscopy observation of the samples crystallized at (T_m − 30)°C: (a) Ny 6, (b) PAE-67 and (c) PAE-48

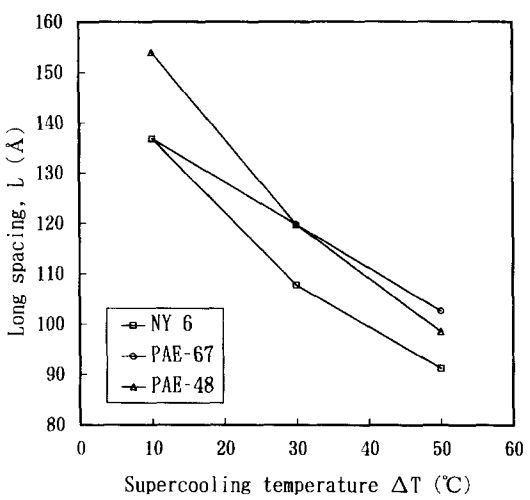

Figure 9 Long spacing of annealed samples as a function of supercooling temperature, $\Delta T = T_m - T_a$

were crystallized at (T_m − 30)°C from their melt. *Figure 8a* shows the well-defined, homogeneous, and nucleated positive spherulites of Ny 6, which is observed by a polarized optical microscope under the cross-polarized condition. On the other hand, the spherulitic texture was not uniform in the specimen of PAE-67; large spherulites were formed in some regions, but were not grown enough in other regions, as shown in *Figure 8b*. In the case of PAE-48, the crystallization seemed to be restricted by the presence of large amounts of soft segments, so that the spherulitic structure became obscure in the whole regions, as shown in *Figure 8c*. This result reveals the low degree of crystallinity and reminds us of the premature crystallites. It may also suggest the extremely small heat fusion in PAE-48 quenched sample, as mentioned above.

SAXS results

Figure 9 shows the long spacing of the annealed samples plotted against the supercooling temperature. The long spacing increases with increase of annealing temperature as usual in every sample but there is a definite difference in the long spacings between Ny 6 and block copolymers, except for the values at $\Delta T = 10$°C, at which PAE-67 might melt partially. The temperature dependence of the long spacing can be explained as the result of the increase of crystal thickness due to the promotion of crystal growth. On the other hand, it is worth noticing the fact that the long spacing of block copolymers is larger than that of Ny 6 at a same ΔT. It is generally considered that the long spacing structure consists of a series of crystalline and amorphous regions in crystalline polymers. In the case of the Ny 6 homopolymer, long spacing is easily assigned. However, in the case of the block copolymer which is composed of nylon 6 hard segments and PPG soft segments, it is important to consider how the soft segment is arranged in the solid structure. As mentioned above, a good compatibility of the soft and hard segments was suggested in the amorphous region. And if the soft segment took part in constituting the amorphous region of the long spacing structure together with the amorphous phase of the hard segment, the long spacing would become larger. Accordingly, these considerations lead us to conclude that the soft segments of block copolymers exist in the intervening amorphous layers between the stacked lamellar crystals[27,28], without making the isolated, separate domains.

CONCLUSIONS

It was found that the PPG soft segments are compatible with the nylon 6 hard segments in the amorphous region of the block copolymers. The hard segment of both block copolymers can crystallize and forms the same crystal structure as nylon 6 homopolymer. In order of Ny 6, PAE-67 and PAE-48, i.e. as the amount of soft segment increases, the melting temperature, crystallinity, and crystal size decrease and the spherulitic structure becomes worse. Especially, a large reduction of crystallinity was observed in PAE-48, in which crystallization seemed to be considerably restricted by a large amount of soft segments. However, the melting point depression could be explained from the concept of 'diluent effect'.

When the samples were annealed, the second lower melting temperature which depended on the annealing temperature appeared in addition to the constant high melting temperature. When the annealing temperature is elevated, the crystal perfection, which may be determined by the supercooling temperature, occurs so as to realize an ideal α-form crystal of nylon 6. Then, it was noticed that the block copolymers of PAE-67 and PAE-48 realized the ideal d_{200} spacing even at high supercooling temperatures, while Ny 6 still did not. The long spacing increases with increase of annealing temperature and the block copolymers always have a larger long spacing than Ny 6 at the same supercooling temperature. It was suggested that the soft segment of block copolymers should exist in the intervening amorphous layers between the stacked lamellar crystals constructing the long spacing structure.

REFERENCES

1. Yu, C. Y. and Jo, W. H., *J. Appl. Polym. Sci.*, 1995, **56**, 895.
2. Zhu, L. L. and Wegner, G., *Makromol. Chem.*, 1981, **182**, 3639.

3. Goldbach, G., Kita, M., Meyer, K. and Richter, K. P., *Progress in Colloid Polym. Sci.*, 1986, **72**, 83.
4. Van Hutten, P. F., Magnus, R. M. and Gaymans, R. J., *Polymer*, 1993, **34**, 4193.
5. Flory, P. J., *Trans. Faraday Soc.*, 1995, **51**, 848.
6. Hoffman, J. D. and Weeks, J. J., *J. Res. Nat. Bur. Stds*, 1962, **A66**, 13.
7. Sorta, E. and Fortuna, G. D., *Polymer*, 1980, **21**, 728.
8. Vallance, M. A. and Cooper, S. L., *Macromolecules*, 1984, **17**, 1208.
9. Castles, J. L., Vallance, M. A., Mckenna, J. M. and Cooper, S. L., *J. Polym. Sci., Polym. Phys. Ed.*, 1985, **23**, 2119.
10. Takahashi, T., Hayashi, N. and Hayashi, S., *J. Appl. Polym. Sci.*, 1996, **60**, 1061.
11. Kohan, M. I., *Nylon Plastics*. John Wiley and Sons, New York, 1973, pp. 303, 330.
12. Wada, Y., *Solid Properties of Polymers* (KOBUNSHI NO KOTAI BUSSEI). Baifukan, Tokyo, 1971, p. 402.
13. Nishio, Y., Hirose, N. and Takahashi, T., *Polym. J.*, 1989, **21**, 347.
14. Prevoserk, D. C., Butler, R. H. and Reimschuessel, H. K., *J. Polym. Sci., Part A-2*, 1971, **9**, 867.
15. Wunderlich, B., *Macromolecular Physics*, Vol. 2. Academic Press Inc., USA, 1976, p. 349.
16. Fakirov, S., Fisher, E. W., Hoffman, R. and Schmidt, G. F., *Polymer*, 1977, **18**, 1121.
17. Lee, L. H., Vanselow, J. J. and Schneider, N. S., *Polym. Engng Sci.*, 1988, **28**, 181.
18. Ogata, N., Yoshimura, F., Yanagawa, T. and Yoshida, K., *Sen-i Gakkaishi*, 1988, **44**, 483.
19. Bankar, V. G., Spruiell, J. E. and White, J. L., *J. Appl. Polym. Sci.*, 1977, **21**, 2341.
20. Murthy, N. S., Bray, R. G., Correale, S. T. and Moore, R. A. F., *Polymer*, 1995, **36**, 3863.
21. Stepaniak, R. F., Garton, A., Carlsson, D. J. and Wiles, D. M., *J. Appl. Polym. Sci.*, 1979, **23**, 1747.
22. Holmes, D. R., Bunn, C. W. and Smith, D. I., *J. Polym. Sci.*, 1955, **17**, 159.
23. Hoashi, K. and Andrews, R. D., *J. Polym. Sci. Part C*, 1972, **38**, 387.
24. Yeh, J. L., Kuo, J. F. and Chen, C. Y., *Materials Chem. Phys.*, 1994, **37**, 161.
25. Hatfield, G. R., Bush, R. W., Killinger, W. E. and Roubicek, P. M., *Polymer*, 1994, **35**, 3943.
26. Gogolewsky, S. and Pennings, A. J., *Polymer*, 1977, **18**, 647.
27. Takahashi, T. and Nagata, F., *J. Macromol. Sci.-Phys.*, 1991, **30**, 25.
28. Zhu, L. L., Wegner, G. and Bandara, U., *Agew. Makromol. Chem.*, 1981, **182**, 3639.